

# New triple molybdate $K_5ScHf(MoO_4)_6$ : Synthesis, Properties, Structure and Phase Equilibria in the $M_2MoO_4-Sc_2(MoO_4)_3-Hf(MoO_4)_2$ ( $M = Li, K$ ) systems

Victoria G. Grossman<sup>a</sup>, Jibzema G. Bazarova<sup>a</sup>, Maksim S. Molokeev<sup>b,c</sup>,

Bair G. Bazarov<sup>a</sup>

<sup>a</sup>*Baikal Institute of Nature Management, Siberian Branch, Russian Academy of Sciences, Sakhyanovoy St., 6, Ulan-Ude 670047, Buryat Republic, Russia*

<sup>b</sup>*Kirensky Institute of Physics, Federal Research Center KSC, Siberian Branch, RAS, 50 / 38 Akademgorodok, Krasnoyarsk 660036, Russia*

<sup>c</sup>*Siberian Federal University, 82 Svobodniy Av., Krasnoyarsk 660041, Russia*  
*E-mail address: grossmanv@mail.ru*

## ABSTRACT

Subsolidus phase relations in the  $M_2MoO_4-Sc_2(MoO_4)_3-Hf(MoO_4)_2$  ( $M = Li, K$ ) systems have been studied by the method of “intersecting cuts”. No new triple molybdates have been identified in the  $Li_2MoO_4-Sc_2(MoO_4)_3-Hf(MoO_4)_2$  system and a new triple molybdate  $K_5ScHf(MoO_4)_6$  is formed in the  $K_2MoO_4-Sc_2(MoO_4)_3-Hf(MoO_4)_2$  system. The structure of  $K_5ScHf(MoO_4)_6$ , have been determined in space group  $R\bar{3}c$  through Rietveld analysis of X-ray powder diffraction data. The melting point of molybdate is 999 K. The compound has high ion conductivity (about  $10^{-3}$  S/cm).

Keywords: Synthesis; Molybdates; X-ray diffraction; DSC; Electrical properties.

## 1. Introduction

The interest to the chemistry of double and triple molybdates during last decades has been maintaining due to their application in science and engineering. Molybdates are well-known and promising as laser materials [1, 2], ferroelectrics and ferroelastics [3, 4], phosphors [5], ionic conductors [6–11], materials for Li(Na)-ion batteries [11, 12] etc. Compounds with open 3D frameworks are considered as promising Na, K- or Li-ion conductors or battery materials [13–20]. For example, ionic conductivities  $10^{-4}-10^{-5}$  S/cm at room temperature were determined for oxides  $Li_3M(MoO_4)_3$  ( $M = Cr, Fe$ ) [21] with Li atoms in large channels, which is comparable to the conductivity of known lithium ion conductors such as  $LiAlSiO_4$  and  $LiSbO_{3.6}$ . The range of complex Mo(VI) oxide phases has been expanding over the during last decades for account of triple molybdates revealed in the course of exploring ternary salt systems [13, 22–30]. A series of  $CsM^{3+}Zr_{0.5}(MoO_4)_3$  compounds with large channels occupied by  $Cs^+$  ions have a significant electrical conductivity of about  $10^{-5}$  S/cm at 800 K with a predominant ionic component above 673 K and average activation energies of 0.3–0.6 eV was measured for  $M = Al, Sc, In$  [29].

The triple molybdates of potassium, trivalent and tetravalent cations were discovered and synthesized [6, 31–33]. These triple molybdates ( $K_5RZr(MoO_4)_6$  ( $R = Al, Cr, Fe, In, Sc$ ) undergo reversible first-order phase transitions at 755–876 K with sharp increase of conductivity up to  $10^{-2}$ – $10^{-3}$   $S \cdot cm^{-1}$  [6]. The open framework, the mobility of cations and the phase transformation were features interesting enough to motivate us to study triple molybdates.

The major task of this work was to search for triple molybdates in  $M_2MoO_4$ – $Sc_2(MoO_4)_3$ – $Hf(MoO_4)_2$  ( $M = Li, K$ ) systems. These systems are attractive primarily for the can be compounds in them with interesting physical properties have been prepared as well as in order to provide a comparison with related systems.

## 2. Experimental

### 2.1. Materials and preparation

Commercially available chemically pure  $MoO_3$ ,  $HfO_2$ ,  $Li_2MoO_4$ ,  $K_2MoO_4$  and high-purity  $Sc_2O_3$  were used as starting materials for the synthesis of simple, double and triple molybdates. Molybdates of scandium and hafnium were synthesized from  $Sc_2O_3$  and  $MoO_3$  at 673–1073 K for 96 h and from  $HfO_2$  and  $MoO_3$  at 673–973 K for 120 h. The starting reactants were well mixed and ground in an agate mortar. For better reactivity, the reaction mixtures were then progressively calcined at the temperatures indicated with intervening by mixing and grinding every 24 h of annealing.

Subsolidus phase relations in the  $M_2MoO_4$ – $Sc_2(MoO_4)_3$ – $Hf(MoO_4)_2$  ( $M = Li, K$ ) systems at 723–823 K were established by the intersecting joins method [34, 35]. Compounds from the boundary systems were preliminarily synthesized, tested for monophasity and used as starting substances for the preparation of samples which served to triangulate isothermal sections.

### 2.2. Characterization

The powder diffraction data of  $K_5ScHf(MoO_4)_6$  for Rietveld analysis was collected at room temperature with a Bruker D8 ADVANCE powder diffractometer (Cu- $K\alpha$  radiation,  $\lambda = 1.5418 \text{ \AA}$ ) and linear VANTEC detector. The step size of  $2\theta$  was  $0.016^\circ$ , and the counting time was 1 s per step. Date analysis was performed using the program TOPAS 4.2.

The thermal property was investigated by the differential scanning calorimetric (DSC) analysis using a NETZSCH STA 449C TG/DSC/DTA thermal analyzer (NETZSCH, Berlin, Germany). A 18 mg sample of powder was placed in a Pt crucible and heated from room temperature at a rate of  $10^\circ K \text{ min}^{-1}$  in an Ar atmosphere.

Electrical conductivity measurements were carried out on cylinder-shaped ceramic samples which were 10 mm in diameter and 2 mm thick, with platinum electrodes by the electrochemical impedance method on a Z-1500J imittance

meter in the temperature range 293–923 K. The test frequency can be set from 1 Hz to 1 MHz at high resolution. Electrical conductivity  $\sigma$  for each temperature was calculated from

$$\sigma = 4h/\pi D^2 R \quad (1)$$

where  $h$  is sample thickness in cm,  $D$  is diameter in cm, and  $R$  is ohmic resistance in  $\Omega$ .

### 3. Results and discussion

The boundary binaries of the  $M_2MoO_4$ – $Sc_2(MoO_4)_3$ – $Hf(MoO_4)_2$  ( $M = Li, K$ ) ternary systems we studied are described in the literature in a sufficiently detailed way [36–48]. It is known that in the  $Li_2MoO_4$ – $Sc_2(MoO_4)_3$  system was found one compound of  $Li_3Sc(MoO_4)_3$  (1:3) composition [36–40]. The compound  $Li_3Sc(MoO_4)_3$ , belongs to the family of isostructural phases  $Li_3R(MoO_4)_3$  ( $R = In, Sc, Fe, Cr, Ga, Al$ ) crystallizing in the orthorhombic structure type of lyonsite  $\alpha$ - $Cu_3Fe_4(VO_4)_6$  [41].

According to Solodovnikov et al. [42], the  $Li_2MoO_4$ – $Hf(MoO_4)_2$  system contains a lithium hafnium molybdate with the composition  $Li_{10-4x}Hf_{2+x}(MoO_4)_9$  ( $0.21 \leq x \leq 0.68$ ). Although it has been suggested in the papers [43, 44] that both compositions  $Li_2Hf(MoO_4)_3$  and  $Li_{10}Hf_2(MoO_4)_9$  are single phases from powder diffraction. Perhaps results can depend on the synthesis conditions. The crystal structure of  $Li_{2.82}Hf_{0.795}Mo_3O_{12}$  is identical to lyonsite-type compounds [41].

According to data [36, 38, 39, 45], three double molybdates of  $KSc(MoO_4)_2$  (1:1),  $K_3Sc(MoO_4)_3$  (3:1), and  $K_5Sc(MoO_4)_4$  (5:1) compositions are formed in the  $K_2MoO_4$ – $Sc_2(MoO_4)_3$  system. The partial non-quasibinarity of the system  $K_2MoO_4$ – $Sc_2(MoO_4)_3$  occurs only in the subsolidus region [40, 46]. This is due to the fact that along with double molybdates, the presence of potassium dimolybdate is recorded in the system. At 723 K, the  $K_2MoO_4$ – $Sc_2(MoO_4)_3$  system become quasi-binary.

The  $K_2MoO_4$ – $Hf(MoO_4)_2$  system contains compounds with the compositions  $K_8Hf(MoO_4)_6$  (4:1) and  $K_2Hf(MoO_4)_3$  (1:1) [47]. No intermediate compounds were found inside the  $Sc_2(MoO_4)_3$ – $Hf(MoO_4)_2$  system [48].

The results of experimental studies of the ternary systems  $M_2MoO_4$ – $Sc_2(MoO_4)_3$ – $Hf(MoO_4)_2$  ( $M = Li, K$ ) at 723–823 K are represented in Fig. 1.

In the  $Li_2MoO_4$ – $Sc_2(MoO_4)_3$ – $Hf(MoO_4)_2$  ternary system, double molybdates  $Li_3Sc(MoO_4)_3$  (1:3) and  $Li_{10-4x}Hf_{2+x}(MoO_4)_9$  ( $0.21 \leq x \leq 0.68$ ) are formed only in two boundary systems and, therefore, is divided by quasi binary joins into three ternary subsystems. For this reason, only these joins was studied in a detailed way in this ternary system (Fig. 1), as well as several points inside secondary triangles.

In addition, the system has the homogeneity region of the phase with the structure of  $Li_{10-4x}Hf_{2+x}(MoO_4)_9$  ( $0.21 \leq x \leq 0.68$ ) lyonsite. Unfortunately, the lithium system is not phase-forming.

Subsolidus phase formation data for the  $Li_2MoO_4$ – $Sc_2(MoO_4)_3$ – $Hf(MoO_4)_2$  ternary system was supplemented with the results of solution-melt crystallization; however, search experiments, too, failed to succeed in preparing triple molybdates

as crystals. The crystallization products under the chosen conditions were crystals of  $\text{Li}_2\text{MoO}_4$  and  $\text{Li}_3\text{Sc}(\text{MoO}_4)_3$  (1:3).

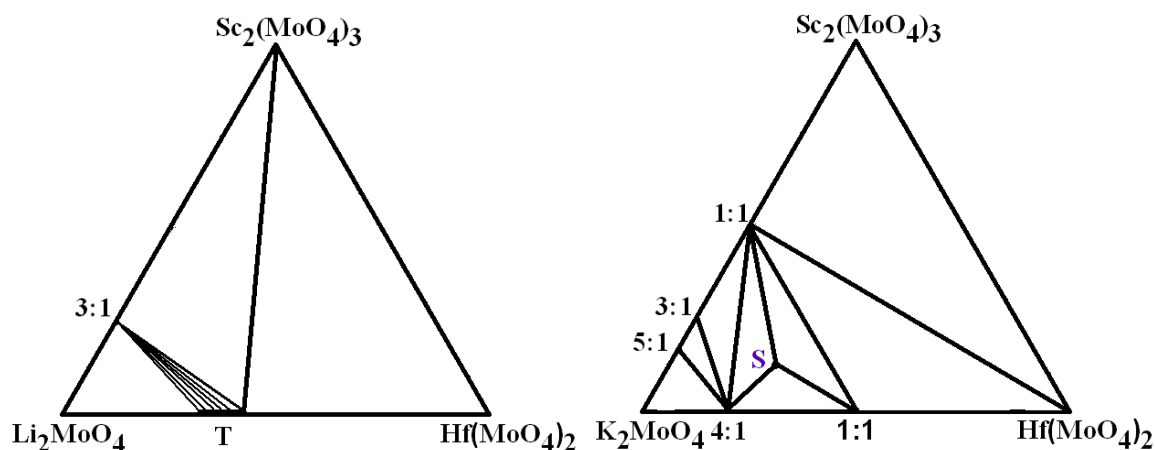


**Fig. 1.** Subsolidus phase relations in the  $\text{M}_2\text{MoO}_4\text{--Sc}_2(\text{MoO}_4)_3\text{--Hf}(\text{MoO}_4)_2$  ( $\text{M} = \text{Li, K}$ ) system at 723–823 K:  $\text{T} = \text{Li}_{10-4x}\text{Hf}_{2+x}(\text{MoO}_4)_9$  ( $0.21 \leq x \leq 0.68$ ),  $\text{S} = \text{K}_5\text{ScHf}(\text{MoO}_4)_6$

The results of the investigation of the  $\text{K}_2\text{MoO}_4\text{--Sc}_2(\text{MoO}_4)_3\text{--Hf}(\text{MoO}_4)_2$  system are presented in Fig. 1. The join  $\text{K}_5\text{Sc}(\text{MoO}_4)_4$  (5:1)– $\text{Hf}(\text{MoO}_4)_2$ , where the new compound  $\text{K}_5\text{ScHf}(\text{MoO}_4)_6$  is formed, was studied with a step of 5–10 mol %, and in the vicinity of a new compound – with a step of 1.5–2.5 mol %. The joins  $\text{K}_5\text{Sc}(\text{MoO}_4)_4\text{--K}_8\text{Hf}(\text{MoO}_4)_6$ ,  $\text{K}_3\text{Sc}(\text{MoO}_4)_3\text{--K}_8\text{Hf}(\text{MoO}_4)_6$ ,  $\text{KSc}(\text{MoO}_4)_2\text{--K}_8\text{Hf}(\text{MoO}_4)_6$ ,  $\text{KSc}(\text{MoO}_4)_2\text{--K}_2\text{Hf}(\text{MoO}_4)_3$ ,  $\text{KSc}(\text{MoO}_4)_2\text{--Hf}(\text{MoO}_4)_2$ ,  $\text{KSc}(\text{MoO}_4)_2\text{--K}_5\text{ScHf}(\text{MoO}_4)_6$ ,  $\text{K}_5\text{ScHf}(\text{MoO}_4)_6\text{--K}_8\text{Hf}(\text{MoO}_4)_6$  and  $\text{K}_5\text{ScHf}(\text{MoO}_4)_6\text{--K}_2\text{Hf}(\text{MoO}_4)_3$  divide the  $\text{K}_2\text{MoO}_4\text{--Sc}_2(\text{MoO}_4)_3\text{--Hf}(\text{MoO}_4)_2$  system into eight subsystems. Molybdate  $\text{K}_5\text{ScHf}(\text{MoO}_4)_6$  was synthesized by annealing in the temperature range of 723–873 K for 100 hours.

All peaks were indexed by trigonal cell ( $R\text{-}3c$ ) with parameters close to  $\text{K}_5\text{InHf}(\text{MoO}_4)_6$  [32]. Therefore this structure was taken as starting model for Rietveld refinement which was performed using TOPAS 4.2 [49]. Two Hf/In sites were occupied by Hf/Sc ions and their occupancies were refined taking into account that sum of occupancies are equal to 1 in each site. In order to reduce number of refined parameters, only one thermal parameter was refined for all O atoms. Refinement was stable and gave low  $R$ -factors (Table 1, Figure 2). Coordinates of atoms and main bond lengths are in Table 2 and Table 3 respectively. The crystal structure of  $\text{K}_5\text{ScHf}(\text{MoO}_4)_6$  is shown in Fig. 3. The structure of trigonal triple molybdate  $\text{K}_5\text{ScHf}(\text{MoO}_4)_6$  is formed by Mo tetrahedrons and two independent (Sc, Hf) octahedrons, which are connected through shared vertexes. Two potassium atoms occupy large voids of the framework.

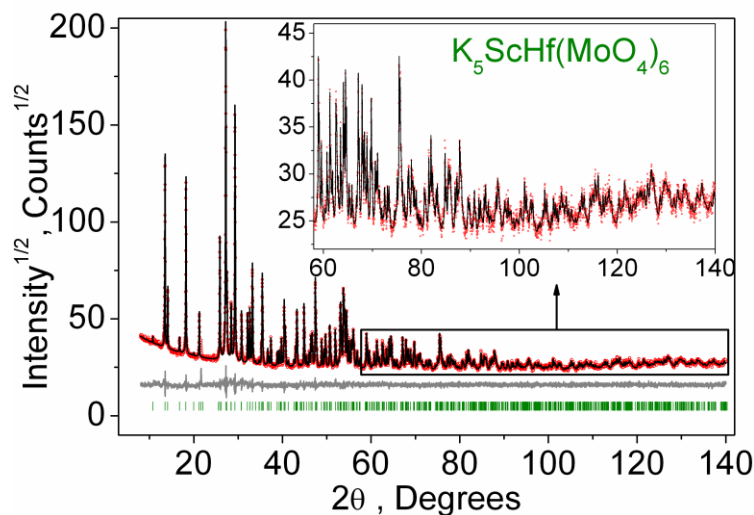


**Fig. 2.** Difference Rietveld plot of  $K_5ScHf(MoO_4)_6$ .

**Table 1.** Main parameters of processing and refinement of the  $K_5ScHf(MoO_4)_6$  sample

Compound	$K_5ScHf(MoO_4)_6$
Sp.Gr.	$R-3c$
$a$ , Å	10.56312 (8)
$c$ , Å	37.6251 (3)
$V$ , Å <sup>3</sup>	3635.74 (6)
$Z$	2
$2\theta$ -interval, °	8-140
$R_{wp}$ , %	4.92
$R_p$ , %	3.77
$R_{exp}$ , %	3.18
$\chi^2$	1.55
$R_B$ , %	1.14

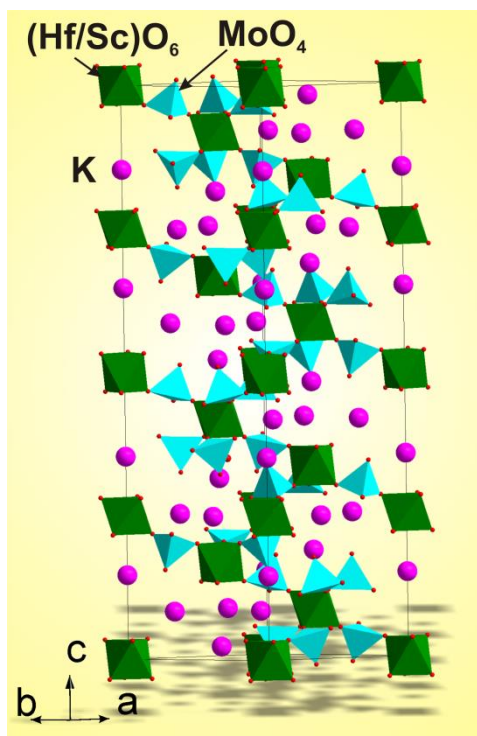
**Table 2.** Fractional atomic coordinates and isotropic displacement parameters (Å<sup>2</sup>) of  $K_5ScHf(MoO_4)_6$

Atom	$x$	$y$	$z$	$B_{iso}$	$Occ.$
Mo	0.34997 (13)	0.05489 (11)	0.03254 (3)	1.05 (7)	1
Hf1	0	0	0	0.66 (9)	0.548 (4)
Sc1	0	0	0	0.66 (9)	0.452 (4)
Hf2	0	0	0.25	0.71 (10)	0.452 (4)
Sc2	0	0	0.25	0.71 (10)	0.548 (4)
K1	0	0	0.35330 (12)	2.13 (13)	1
K2	0.3852 (4)	0	0.25	3.51 (13)	1
O1	0.1658 (8)	0.0279 (9)	0.03393 (19)	1.23 (12)	1
O2	0.4835 (9)	0.2315 (8)	0.05139 (17)	1.23 (12)	1
O3	0.3498 (9)	-0.0920 (9)	0.05349 (18)	1.23 (12)	1
O4	0.3972 (7)	0.0604 (7)	-0.01022 (18)	1.23 (12)	1

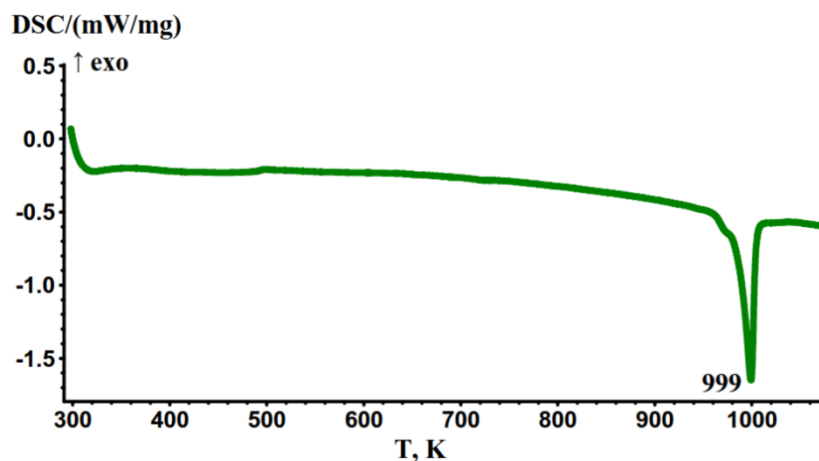
**Table 3.** Main bond lengths (Å) of  $K_5ScHf(MoO_4)_6$ 

Mo—O1	1.821 (4)	K1—O3 <sup>ii</sup>	2.771 (7)
Mo—O2	1.828 (7)	K1—O4 <sup>i</sup>	2.889 (6)
Mo—O3	1.739 (7)	K2—O2 <sup>i</sup>	3.075 (7)
Mo—O4	1.677 (7)	K2—O3 <sup>iii</sup>	2.979 (7)
(Hf1/Sc1)—O1	2.066 (7)	K2—O4 <sup>ii</sup>	2.823 (7)
(Hf2/Sc2)—O2 <sup>i</sup>	2.065 (7)		

Symmetry codes: (i)  $-x+2/3, -y+1/3, -z+1/3$ ; (ii)  $-x+y+2/3, -x+1/3, z+1/3$ ; (iii)  $y+2/3, -x+y+1/3, -z+1/3$

**Fig. 3.** Crystal structure of  $K_5ScHf(MoO_4)_6$ .

According to the DSC measurements shown in Fig. 4, the obtained molybdate does not possess phase transitions over the temperature range of 300–1060 K and melts at 999 K.

**Fig. 4.** Differential scanning calorimetric scans of the  $K_5ScHf(MoO_4)_6$

Keeping in mind that from structural point of view the K molybdate are favorable for potassium-ion transport, we studied electric conduction properties of this phase.

We have plotted impedance diagrams viz., ReZ (pure resistive part of the impedance) versus ImZ (capacitive reactance). A typical impedance Nyquist spectrum of a solid electrolyte material may include arcs corresponding to the grain bulk, grain boundary, electrode-related impedance.

As shown, the impedance spectrum measured at 643 K (Fig. 5a) exhibits two independent semicircular arcs and a straight line from high frequency to low frequency, which corresponds to the conduction across the bulk, the conduction across grain boundary and the impedance response corresponding to electrode, respectively. With the increasing of temperature, the arc corresponds to the grain contributions gradually disappearing, and the arc or spike corresponds to the grain boundary and electrode shifted to higher frequencies as shown in the impedance spectrum measured at 753 and 803 K (Fig. 5b,c). When the temperature is beyond 853 K, the increase of arc corresponding to the contribution of the electrode is observed, which indicates that the ion could diffuse through the entire thickness of bulk and grain boundary (Fig. 5c).

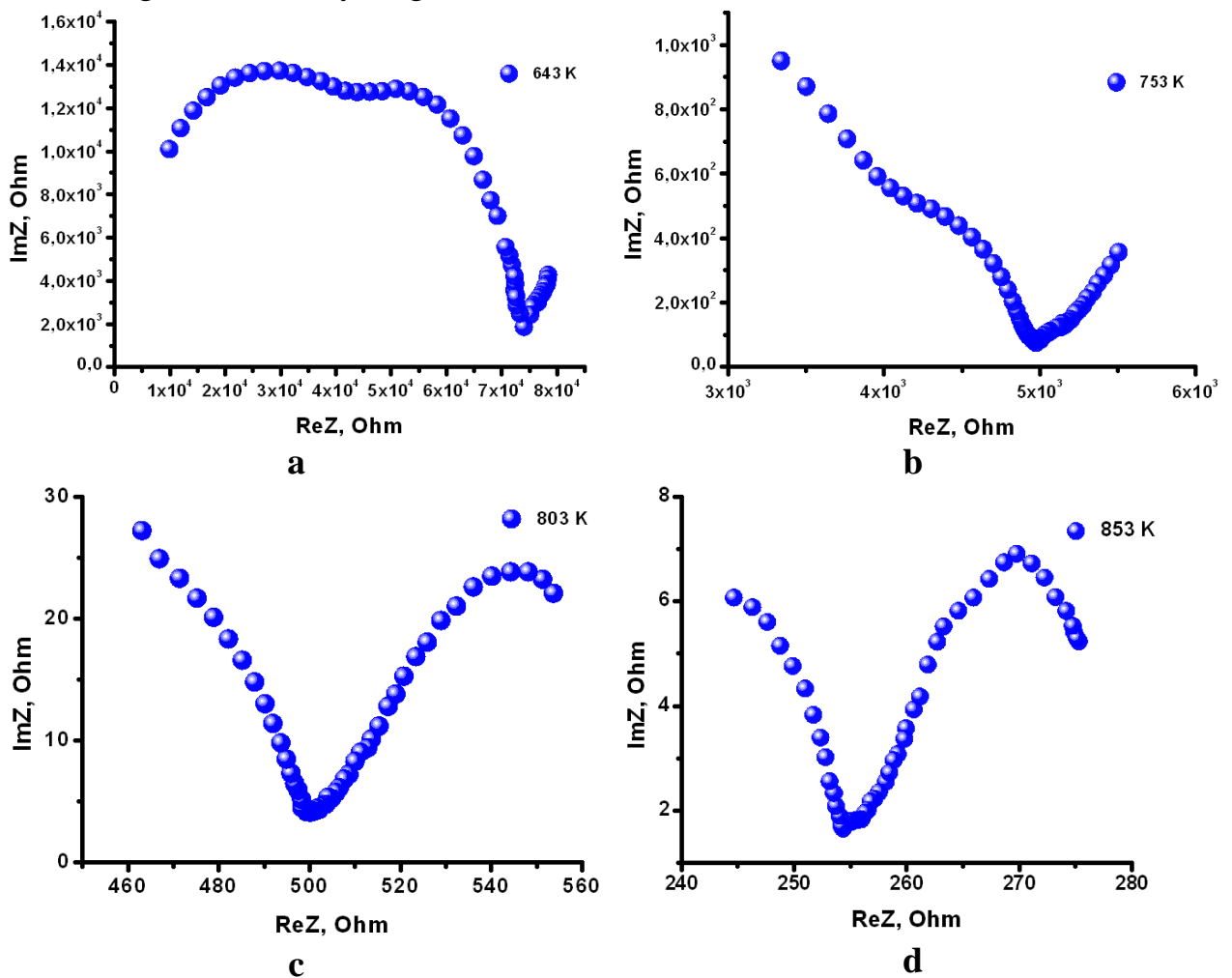


**Fig. 5.** The impedance profiles for  $K_5ScHf(MoO_4)_6$  molybdate measured at different temperatures

The corresponding conductivity is converted by the resistance  $R$  using

$$\sigma = 4h/\pi D^2 R \quad (1)$$

where  $h$  is sample thickness in cm,  $D$  is diameter in cm, and  $R$  is ohmic resistance in  $\Omega$ .

In Fig. 6 the variation of ac conductivity ( $\sigma$ ) with  $1000/T$  at various frequencies and with  $\omega$  (at various temperatures) are presented for  $K_5ScHf(MoO_4)_6$ .

At high temperatures, the conductivity curves do not depend significantly on frequency, with their temperature behavior obeying the Arrhenius law. This law is known to be typical for conductivity in most solid electrolytes, and may be considered as an indication of ionic transport in  $K_5ScHf(MoO_4)_6$ . The temperature dependence of electrical conductivity in  $K_5ScHf(MoO_4)_6$  shows a kink appears on the curve at 770 K. As seen from (Fig. 6), the conductivity on heating accompanies fall on cooling. These effects are separated by thermal hysteresis of about 100 K. Although there is no phase transition on the DSC curve (Fig. 4). The 900 K conductivity of the compound  $K_5ScHf(MoO_4)_6$  is  $10^{-3} S \cdot cm^{-1}$ , and comparable with those for  $K_5RZr(MoO_4)_6$  ( $R = Al, Cr, Fe, In, Sc$ ) [6],  $Na_{1-x}Mg_{1-x}Sc_{1+x}(MoO_4)_3$  ( $0 \leq x \leq 0.5$ ) [50],  $Na_{25}Cs_8R_5(MoO_4)_{24}$  ( $R = Sc, In$ ) [15],  $K_{1-x}A_{1-x}R_{1+x}(MoO_4)_3$  ( $0 \leq x \leq 0.5$ ) ( $A = Mg, Mn, Co, Ni; R = Sc, Yb, Lu$ ) [51],  $Rb_5TmHf(MoO_4)_6$  [10]. Below 600 K, the conductivity data demonstrate behavior depending on frequency. From Fig. 6b shows that conductivity of  $K_5ScHf(MoO_4)_6$  gradually increases with the increase of frequency of applied alternating electric field. This is mainly attributed as the enhanced migration of the ions through grain boundaries.

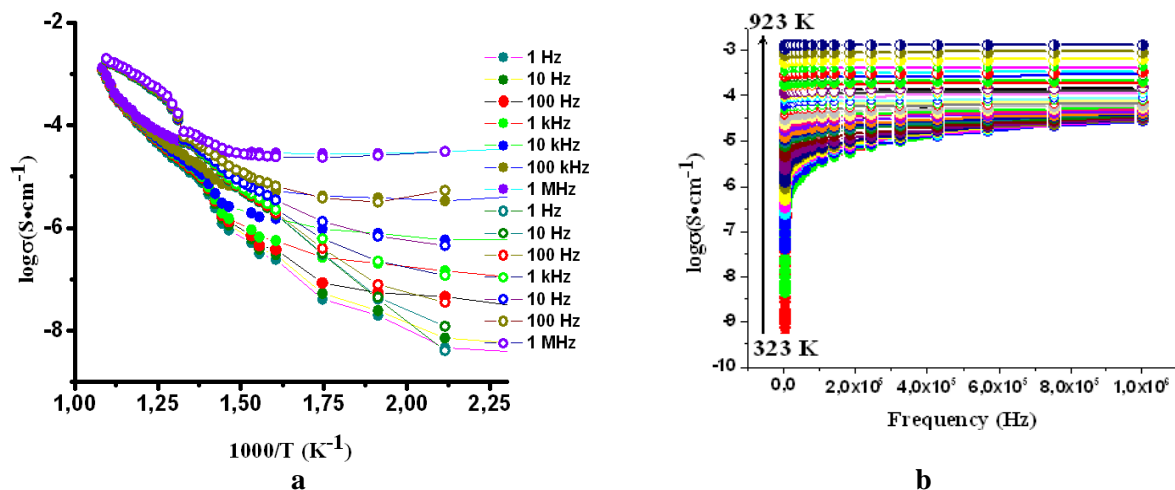


**Fig. 6.** Variation in ac conductivity with  $1000/T$  at different frequencies (a; triangles – heating, circles – cooling) and (b) with frequency at different temperatures for the sample  $K_5ScHf(MoO_4)_6$

#### 4. Conclusions

Our study of chemical interactions in the system  $K_2MoO_4$ – $Sc_2(MoO_4)_3$ – $Hf(MoO_4)_2$  by means of solid state reactions us to reveal a new triple molybdate  $K_5ScHf(MoO_4)_6$ .

It was found that triple molybdates are not formed in the lithium-containing system. The unit cell parameters were precisely determined for  $K_5ScHf(MoO_4)_6$ . This molybdate crystallizes in a trigonal structure, space group  $R\bar{3}c$ . The



electrophysical and thermal properties of molybdate have been studied. Molybdate under study is characterized with ionic conductivity of the  $1 \times 10^{-8}$ – $10^{-3}$  S·cm<sup>-1</sup> at 445–900 K. The high conductivity of K<sub>5</sub>ScHf(MoO<sub>4</sub>)<sub>6</sub> molybdate allows us to consider it as promising solid electrolyte. The K<sub>5</sub>ScHf(MoO<sub>4</sub>)<sub>6</sub> compound was found to melt at 999 K.

### Acknowledgments

This study was carried out within the state assignment of FASO of Russia (Theme No 0339-2016-0007) as well was supported by RFBR Grants 18-08-00799 and 18-03-00557.

### References

- [1] D. Lu, X. Gong, Y. Chen, J. Huang, Y. Lin, Z. Luo, Y. Huang, Synthesis and photoluminescence characteristics of the LiGd<sub>3</sub>(MoO<sub>4</sub>)<sub>5</sub>: Eu<sup>3+</sup> red phosphor with high color purity and brightness, *Opt. Mater. Express.* 8 (2018) 259–269. <https://doi.org/10.1364/OME.8.000259>.
- [2] G.Q. Wang, L.Y. Li, Y.N. Feng, H.Yu, X. H. Zheng, Tb<sup>3+</sup>- and Yb<sup>3+</sup>-doped novel KBaLu(MoO<sub>4</sub>)<sub>3</sub> crystals with disordered chained structure showing down- and up-conversion luminescence, *Cryst. Eng. Comm.* 20 (2018) 3657–3665. <https://doi.org/10.1039/C8CE00461G>.
- [3] M.B. Zapart, W. Zapart, M. Maczka, Complex ferroelastic domain patterns of K<sub>1-x</sub>Rb<sub>x</sub>Sc(MoO<sub>4</sub>)<sub>2</sub> crystals, *Ferroelectrics.* 1 (2016) 34–41. <https://doi.org/10.1080/00150193.2016.1160729>.
- [4] W. Zapart, M.B. Zapart, Phase Transitions in Ferroelastic RbIn(MoO<sub>4</sub>)<sub>2</sub> at 163 and 143 K, *Ferroelectrics.* 1 (2013) 116–120. <https://doi.org/10.1080/00150193.2013.839289>.
- [5] G. Benoît, J. Véronique, A. Arnaud, G. Alain, Luminescence properties of tungstates and molybdates phosphors: illustration on ALn(MO<sub>4</sub>)<sub>2</sub> compounds (A = alkaline cation, Ln = lanthanides, M = W, Mo), *Solid State Sci.* 13 (2011) 460–467. <https://doi.org/10.1016/j.solidstatesciences.2010.12.013>.
- [6] J.G. Bazarova, A.V. Logvinova, B.G. Bazarov, Y.L. Tushinova, S.G. Dorzhieva, J. Temujin, Synthesis of new triple molybdates K<sub>5</sub>RZr(MoO<sub>4</sub>)<sub>6</sub> (R = Al, Cr, Fe, In, Sc) in the K<sub>2</sub>MoO<sub>4</sub>–R<sub>2</sub>(MoO<sub>4</sub>)<sub>3</sub>–Zr(MoO<sub>4</sub>)<sub>2</sub> systems, their structure and electrical properties, *J. Alloy. Compd.* 741 (2018) 834–839. <https://doi.org/10.1016/j.jallcom.2018.01.208>.
- [7] K.M. Begama, Y.H. Taufiq-Yap, M.S. Michael, S.R.S. Prabaharana, A new NASICON-type polyanion, Li<sub>x</sub>Ni<sub>2</sub>(MoO<sub>4</sub>)<sub>3</sub> as 3-V class positive electrode material for rechargeable lithium batteries, *Solid State Ionics.* 172 (2004) 47–52. <https://doi.org/10.1016/j.ssi.2004.01.037>.
- [8] N.M. Kozhevnikova, I.Yu. Kotova, X-ray diffraction study of phases of variable composition M<sub>1-x</sub>A<sub>1-x</sub>R<sub>1+x</sub>(MoO<sub>4</sub>)<sub>3</sub> (0 ≤ x ≤ 0.3–0.5) with M = Na or K; A = Mg, Mn, Co, or Ni; and R = Al, In, Cr, Fe, Sc, Zr. *Neorg. Khimii.* 45 (2000) 102–103.
- [9] J. Galy, Ph. Salles, P. Rozier, A. Castro, Anionic conductors Ln<sub>2/3</sub>[Bi<sub>12</sub>O<sub>14</sub>](MoO<sub>4</sub>)<sub>5</sub> with Ln = La, Nd, Gd, Ho, Yb. Synthesis-spark plasma sintering-structure-electric properties, *Solid State Ionics.* 177 (2006) 2897–2902. <https://doi.org/10.1016/j.ssi.2006.07.059>.
- [10] O.D. Chimitova, B.G. Bazarov, K.N. Fedorov, Zh.G. Bazarova, Electrical Properties of Triple Molybdates Rb<sub>3</sub>LnHf(MoO<sub>4</sub>)<sub>6</sub>, *Russ. J. Appl. Chem.* 81 (2008) 1928–1929. <https://doi.org/10.1134/S1070427208110335>.
- [11] I. Jendoubi, R.B. Smail, M. Maczka, M.F. Zid, Optical and electrical properties of the yavapaiite-like molybdate NaAl(MoO<sub>4</sub>)<sub>2</sub>, *Ionics.* 24 (2018) 3515–3533. <https://doi.org/10.1007/s11581-018-2490-x>.

- [11] D. Mikhailova, A. Sarapulova, A. Voss, A. Thomas, S. Oswald, W. Gruner, D.M. Trots, N.N. Bramnik, H. Ehrenberg,  $\text{Li}_3\text{V}(\text{MoO}_4)_3$ : A new material for both Li extraction and insertion, *Chem. Mater.* 22 (2010) 3165–3173. <https://doi.org/10.1021/cm100213a>.
- [12] J. Gao, P. Zhao, K. Feng,  $\text{Na}_{2.67}\text{Mn}_{1.67}(\text{MoO}_4)_3$ : A 3.45 V alluaudite-type cathode candidate for sodium-ion batteries, *Chem. Mater.* 29 (2017) 940–944. <https://doi.org/10.1021/acs.chemmater.6b05308>.
- [13] V.N. Yudin, E.S. Zolotova, S.F. Solodovnikov, Z.A. Solodovnikova, I.V. Korolkov, S.Yu. Stefanovich, B.M. Kuchumo, Synthesis, Structure, and Conductivity of Alluaudite-Related Phases in the  $\text{Na}_2\text{MoO}_4$ – $\text{Cs}_2\text{MoO}_4$ – $\text{CoMoO}_4$  System, *Eur. J. Inorg. Chem.* (2019) 277–286. <https://doi.org/10.1002/ejic.201801307>.
- [14] M. Niazmand, Z. Khakpour, A. Mortazavi, Electrochemical properties of nanostructure NASICON synthesized by chemical routes: A comparison between coprecipitation and sol-gel, *J. Alloy. Compd.* 798 (2019) 311–319. <https://doi.org/10.1016/j.jallcom.2019.05.170>.
- [15] A.A. Savina, S.F. Solodovnikov, D.A. Belov, Z.A. Solodovnikova, S.Yu. Stefanovich, B.I. Lazoryakd, E.G. Khaikina, New alluaudite-related triple molybdates  $\text{Na}_{25}\text{Cs}_8\text{R}_5(\text{MoO}_4)_{24}$  (R = Sc, In): synthesis, crystal structures and properties, *New J. Chem.* 41 (2017) 5450–5457. <https://doi.org/10.1039/C7NJ00202E>
- [16] I. Ennajeh, S. Georges, Y.B. Smida, A. Guesmi, M.F. Zid, H. Boughazala, Synthesis, crystal structure, sintering and electrical properties of a new alluaudite-like triple molybdate  $\text{K}_{0.13}\text{Na}_{3.87}\text{MgMo}_3\text{O}_{12}$ , *RSC Adv.* 5 (2015) 38918–38925. <https://doi.org/10.1039/C5RA02276B>
- [17] S. Patoux, C. Wurm, M. Morcrette, G. Rousse, C. Masquelier, A Comparative Structural and Electrochemical Study of Monoclinic  $\text{Li}_3\text{Fe}_2(\text{PO}_4)_3$  and  $\text{Li}_3\text{V}_2(\text{PO}_4)_3$ , *J. Power Sources.* 119–121 (2003) 278–284. [https://doi.org/10.1016/S0378-7753\(03\)00150-2](https://doi.org/10.1016/S0378-7753(03)00150-2).
- [18] A.S. Andersson, B. Kalska, P. Eyob, D. Aernout, L. Haggstrom, J.O. Thomas, Lithium insertion into rhombohedral  $\text{Li}_3\text{Fe}_2(\text{PO}_4)_3$ , *Solid State Ionics.* 140 (2001) 63–70. [https://doi.org/10.1016/S0167-2738\(01\)00694-4](https://doi.org/10.1016/S0167-2738(01)00694-4).
- [19] J. Gaubicher, C. Wurm, G. Goward, C. Masquelier, L. Nazar, Rhombohedral Form of  $\text{Li}_3\text{V}_2(\text{PO}_4)_3$  as a Cathode in Li-Ion Batteries, *Chem. Mater.* 12 (2000) 3240–3242. <https://doi.org/10.1021/cm000345g>.
- [20] K.M. Begam, M.S. Michael, Y.H. Taufiq-Yap, New Lithiated NASICON-Type  $\text{Li}_2\text{Ni}_2(\text{MoO}_4)_3$  for Rechargeable Lithium Batteries Synthesis, Structural, and Electrochemical Properties, S.R.S. Prabaharan, *Electrochem. Solid-State Lett.* 7 (2004) A242–A246. <https://doi.org/10.1149/1.1760711>
- [21] L. Sebastian, Y. Piffard, A.K. Shukla, F. Taulelle, J. Gopalakrishnan, Synthesis, structure and lithium-ion conductivity of  $\text{Li}_{2-2x}\text{Mg}_{2+x}(\text{MoO}_4)_3$  and  $\text{Li}_3\text{M}(\text{MoO}_4)_3$  (M(III) = Cr, Fe), *J. Mater. Chem.* 13 (2003) 1797–1802. <https://doi.org/10.1039/B301189E>
- [22] V.G. Grossman, B.G. Bazarov, Zh.G. Bazarova, Subsolidus phase diagrams for the  $\text{Tl}_2\text{MoO}_4$ – $\text{Ln}_2(\text{MoO}_4)_3$ – $\text{Hf}(\text{MoO}_4)_2$  systems, where Ln = La–Lu, *Rus. J. Inorg. Chem.* 53 (2008) 1788–1794. <https://doi.org/10.1134/S003602360811020X>.
- [23] N.M. Kozhevnikova, S.Yu. Batueva, Phase Formation in the System  $\text{Li}_2\text{MoO}_4$ – $\text{MgMoO}_4$ – $\text{Sc}_2(\text{MoO}_4)_3$ , *Rus. J. Inorg. Chem.* 61 (2016) 1379–1382. <https://doi.org/10.1134/S0036023616100120>.
- [24] O.A. Gulyaeva, Z.A. Solodovnikova, S.F. Solodovnikov, V.N. Yudin, E.S. Zolotova, V.Yu. Komarov, Subsolidus phase relations and structures of solid solutions in the systems  $\text{K}_2\text{MoO}_4$ – $\text{Na}_2\text{MoO}_4$ – $\text{MMoO}_4$  (M = Mn, Zn), *J. Solid State Chem.* 272 (2019) 148–156. <https://doi.org/10.1016/j.jssc.2019.02.010>.
- [25] B.G. Bazarov, R.F. Klevtsova, Ts.T. Bazarova, L.A. Glinskaya, K.N. Fedorov, A.D. Tsyrendorzhieva, O.D. Chimitova, Zh.G. Bazarova, Phase equilibria in the systems  $\text{Rb}_2\text{MoO}_4$ – $\text{R}_2(\text{MoO}_4)_3$ – $\text{Hf}(\text{MoO}_4)_2$  (R = Al, In, Sc, Fe(III)) and the crystal structure of double molybdate  $\text{RbFe}(\text{MoO}_4)_2$ , *Rus. J. Inorg. Chem.* 51 (2006) 1111–1115. <https://doi.org/10.1134/S0036023606070151>.

- [26] I.Yu. Kotova, S.F. Solodovnikov, Z.A. Solodovnikova, D.A. Belov, S.Yu. Stefanovich, A.A. Savina, E.G. Khaikina, New series of triple molybdates  $\text{AgA}_3\text{R}(\text{MoO}_4)_5$  ( $\text{A} = \text{Mg}$ ,  $\text{R} = \text{Cr}$ ,  $\text{Fe}$ ;  $\text{A} = \text{Mn}$ ,  $\text{R} = \text{Al}$ ,  $\text{Cr}$ ,  $\text{Fe}$ ,  $\text{Sc}$ ,  $\text{In}$ ) with framework structures and mobile silver ion sublattices, *J. Solid State Chem.* 238 (2016) 121–128. <https://doi.org/10.1016/j.jssc.2016.03.003>.
- [27] K.M. Khal'baeva, S.F. Solodovnikov, E.G. Khaikina, Y.M. Kadyrova, Z.A. Solodovnikova, O.M. Basovich, Phase formation in the  $\text{Li}_2\text{MoO}_4\text{--K}_2\text{MoO}_4\text{--In}_2(\text{MoO}_4)_3$  system and crystal structures of new compounds  $\text{K}_3\text{InMo}_4\text{O}_{15}$  and  $\text{LiK}_2\text{In}(\text{MoO}_4)_3$ , *J. Solid State Chem.* 187 (2012) 276–281. <https://doi.org/10.1016/j.jssc.2012.01.010>.
- [28] B.G. Bazarov, R.F. Klevtsova, A.D. Tsyrendorzhieva, L.A. Glinkaaya, Zh.G. Bazarova, Crystalline structure of triple molybdate  $\text{Rb}_5\text{FeHf}(\text{MoO}_4)_6$  – a new phase in the system  $\text{Rb}_2\text{MoO}_4\text{--Fe}_2(\text{MoO}_4)_3\text{--Hf}(\text{MoO}_4)_2$ , *J. Struct. Chem.* 45 (2001) 1038–1043. <https://doi.org/10.1007/s10947-005-0091-9>.
- [29] B.G. Bazarov, T.V. Namsaraeva, K.N. Fedorov, Zh. G. Bazarova, Subsolidus phase diagrams of the systems  $\text{Cs}_2\text{MoO}_4\text{--R}_2(\text{MoO}_4)_3\text{--Zr}(\text{MoO}_4)_2$ , where  $\text{R} = \text{Al}$ ,  $\text{Sc}$ , or  $\text{In}$ , *Russ. J. Inorg. Chem.* 52 (2007) 1454–1458. <https://doi.org/10.1134/S0036023607090240>.
- [30] V.G. Grossman, B.G. Bazarov, R.F. Klevtsova, L.A. Glinskaya, Zh.G. Bazarova, Phase equilibria in the  $\text{Tl}_2\text{MoO}_4\text{--Fe}_2(\text{MoO}_4)_3\text{--Hf}(\text{MoO}_4)_2$  system and the crystal structure of ternary molybdate  $\text{Tl}(\text{FeHf}_{0.5})(\text{MoO}_4)_3$ , *Russ. Chem. Bull.* 61 (2012) 1546–1549. <https://doi.org/10.1007/s11172-012-0202-7>.
- [31] E.Yu. Romanova, B.G. Bazarov, R.F. Klevtsova, L.A. Glinskaya, Yu.L. Tushinova, K.N. Fedorov, Zh.G. Bazarova, Phase formation in the  $\text{K}_2\text{MoO}_4\text{--Lu}_2(\text{MoO}_4)_3\text{--Hf}(\text{MoO}_4)_2$  system. Crystal structure study of triple molybdate  $\text{K}_5\text{LuHf}(\text{MoO}_4)_6$ , *J. Inorg. Chem.* 52 (2007) 815–818. <https://doi.org/10.1134/S0036023607050154>.
- [32] B.G. Bazarov, Ts.T. Bazarova, K.N. Fedorov, Zh.G. Bazarova, R.F. Klevtsova, L.A. Glinskaya, Synthesis and crystal structure of triple molybdate  $\text{K}_5\text{InHf}(\text{MoO}_4)_6$ , *Russ. J. Inorg. Chem.* 50 (2005) 1240–1243.
- [33] J.G. Bazarova, Yu.L. Tushinova, V.G. Grossman, Ts.T. Bazarova, B.G. Bazarov, R.V. Kurbatov, Phase relations in the  $\text{Me}_2\text{MoO}_4\text{--In}_2(\text{MoO}_4)_3\text{--Hf}(\text{MoO}_4)_2$  systems, where  $\text{Me} = \text{Li}$ ,  $\text{K}$ ,  $\text{Tl}$ ,  $\text{Rb}$ ,  $\text{Cs}$ , *Chimica Techno Acta.* 5 (2018) 126–131. <https://doi.org/10.15826/chimtech.2018.5.3.01>
- [34] W.Z. Guertler, Zur Fortentwicklung der Konstitutionsforschungen bei ternaren Systemen, *Anorg. Allg. Chem. Bd.* 154 (1926) 439–455.
- [35] L. Niepel, M. Malinovsky, Triangulation of phase diagrams, *Chem. Zvesti*, 32 (1978) 810–820.
- [36] Yu.A. Velikodny, Abstract of the dissertation ... Candidate of Chemical Sciences, Moscow, 1975, 17 p [in Russian].
- [37] P.V. Klevtsov, Synthesis of the crystal and the study of some double Li, R-molybdates for  $\text{R}^{3+} = \text{Fe}$ ,  $\text{Al}$ ,  $\text{Sc}$ ,  $\text{Ga}$  and  $\text{In}$ , *Sov. Phys. Crystallogr. (Engl. Transl.)* 15 (1970) 682–685.
- [38] V.K. Trunov, V.A. Efremov, Yu.A. Velikodny, Crystal chemistry and properties of double molybdates and tungstates, Leningrad (USSR): Nauka, 1986.
- [39] L.N. Komissarova, V.K. Trunov, N.P. Anoshina, L.A. Nesterova, B.M. Shatsky, Double molybdates and scandium tungstates and alkali metals, *Inorg. Mater.* 6 (1970) 1025–1027.
- [40] Yu.M. Kadyrova, Abstract of the dissertation ... Candidate of Chemical Sciences, Irkutsk, 2010, 24p [in Russian].
- [41] J.P. Smith, P.C. Stair, K.R. Poeppelmeier, The Adaptable Lyonsite Structure, *Chem. Eur. J.* 12 (2006) 5944–5953. <https://doi.org/10.1002/chem.200600294>
- [42] S.F. Solodovnikov, L.V. Balsanova, B.G. Bazarov, E.S. Zolotova, Zh.G. Bazarova, Phase formation in the  $\text{Rb}_2\text{MoO}_4\text{--Li}_2\text{MoO}_4\text{--Hf}(\text{MoO}_4)_2$  system and the crystal structure of  $\text{Rb}_5(\text{Li}_{1/3}\text{Hf}_{5/3})(\text{MoO}_4)_6$ , *Russ. J. Inorg. Chem.* 48 (2003) 1084–1088.
- [43] V.K. Trunov, About double molybdates of alkali and alkaline earth elements, *Zh. Neorg. Khim.* 16 (1971) 553–554.

- [44] P.V. Klevtsov, E.S. Zolotova, Crystallization from a solution in the melt of  $\text{Li}_2\text{O}-\text{MoO}_3$  and some properties of zirconium, hafnium and titanium molybdates, *Izv. Akad. Nauk SSSR Neorg. Mater.* 9 (1973) 79–82.
- [45] R.F. Klevtsova, P.V. Klevtsov, Synthesis and crystal structure of the double molybdates  $\text{KR}(\text{MoO}_4)_2$  for  $\text{R}^{3+} = \text{Al}, \text{Sc},$  and  $\text{Fe}$ , and of the tungstate  $\text{KSc}(\text{WO}_4)_2$ , *Sov. Phys. Crystallogr.* (Engl. Transl.) 15 (1970) 953–959.
- [46] E.G. Khaikina, Abstract of the dissertation ... Doctor of Chemical Sciences, Novosibirsk, 2008, 39p [in Russian].
- [47] E.S. Zolotova, Abstract of the dissertation ... Candidate of Chemical Sciences, Novosibirsk, 1986, 25 p [in Russian].
- [48] Yu.L. Tushinova, J.G. Bazarova, S.I. Arhincheeva, Phase equilibria in  $\text{R}_2(\text{MoO}_4)_3-\text{Zr}(\text{MoO}_4)_2$  systems. All-Russian Scientific Conf. with Int. Partic. (Ulan-Ude: BSC SB RAS Press) (2002) 90–91.
- [49] Bruker AXS TOPAS V4: General profile and structure analysis software for powder diffraction data. – User's Manual. Bruker AXS, Karlsruhe, Germany. 2008.
- [50] N.M. Kozhevnikova, S.Yu. Tsyretarova, Synthesis and study of the phase formation in the  $\text{Na}_2\text{MoO}_4-\text{MgMoO}_4-\text{Sc}_2(\text{MoO}_4)_3$  system, *Russ. J. Inorg. Chem.* 60 (2015) 520–525. <https://doi.org/10.1134/S0036023615040087>.
- [51] Kozhevnikova, N.M. and Mosokhoyev, M.B., Ternary molybdates (Ternary Molybdates), Ulan-Ude: Buryat. Gos. Univ., 2000.